Performance optimization of the LTS$_N$ method

Roberto P. Souto^{a1}, Haroldo F. Campos Velho ^{b} and Stephan Stephany^{b}

^{a}National Laboratory for Scientific Computing, Petrópolis, RJ, Brazil
^{b}National Institute for Space Research, São José dos Campos, SP, Brazil

Abstract

This paper presents the computational performance of some direct and iterative methods for solving a sparse linear system generated by the LTS$_N$ solver of the radiative transfer equation (RTE). A case study was performed for a hydrologic optics problem, where the RTE simulates the interaction of visible light in water, yielding radiation intensity values (radiances) in different angles, for each level of depth. The case study is related to a non-homogeneous medium with a high degree of anisotropy, calculating the radiance at various depth levels, resulting in a sparse system with 12000 unknowns (radiances). Execution times of two direct method (LU factorization) and two iterative method (GMRES) were compared. These methods were implemented as non-commercial and open source packages. The two direct methods were implemented using the LAPACK and MUMPS packages, designed respectively for dense and sparse systems, were used. The two iterative methods were implemented using libraries LIS and CUSP, designed for CPU and GPU architectures, respectively. Computational performance of the four methods is presented and discussed as well the accuracy of the numerical solutions.

Keywords: radiative transfer equation, hydrologic optics, sparse linear systems, direct methods, iterative methods, inverse problems, GPU computing.

1   Introduction

The radiative transfer equation (RTE) is a mathematical model for the study of absorption, transmission, and scattering of photons in a medium. This work employs the RTE in a hydrologic optics problem that involves the determination of the radiance distribution in a body of water, given the boundary conditions, source term, inherent optical properties, such as the absorption a and scattering b coefficients, and the scattering phase function.

---

[1]E-mail Corresponding Author: rpsouto@lncc.br

A brief description of the RTE components is given in the beginning of Section 2.

This work also employs bio-optical models that correlate coefficients a and b to the chlorophyll-a concentration profile. The spatial domain is discretized in a number of regions (R), being the chlorophyll-a concentration assumed as constant in each region. The discrete chlorophyll-a profile is then defined by ($R + 1$) points.

One method for solving the RTE is given by the discrete ordinates equations, or S_N equations. In such scheme, the RTE is decoupled in N azimuthal modes, each one solved independently. Here, it is employed a version of S_N method, the LTS_N method [4, 8], which applies the Laplace transform to the S_N ordinates. The LTS_N method emerged in the early 1990s as a result of research on transport of neutrons, and was further extended to radiative transfer problems.

In a medium with high degree of anisotropy like a natural body of water, there is a big number of possible scattering directions that require radiance calculations. In the case of a non-homogeneous medium containing many regions with different optical properties according to the depth, such calculation of radiances is replicated to all discrete depth levels of the vertical domain. In such a scenario, the LTS_N formulation yields a sparse matrix system, in which the radiances are calculated in different directions, for each depth level. Details of the discrete ordinate formulation, and how LST_N method solves it, is presented in Subsection 2.1 and in Subsection 2.2.

The chosen case study refers to a hydrologic optics problem with 150 azimuthal directions and 80 depths, which requires the solving of a sparse linear system with 12,000 unknowns. Such a large system requires th euse of a proper numerical library in order to optimize the computational performance of the LTS_N method. In this scope, two direct and two iterative methods were evaluated.

Originally, computer codes for the LTS_N method include solvers for dense matrices such as the one of the LAPACK (Linear Algebra Package) library. The performance of such solver, taken as reference, is compared to the following solvers that are specific for sparse systems: i) the direct method implemented in the MUMPS (MUltifrontal MassivelyParallel sparse direct Solver) package; ii) the iterative GMRES (Generalized Minimal Residual) method implemented in LIS (Library of Iterative Solvers); and iii) the iterative GMRES method implemented in CUSP library, intended for GPU (general purpose Graphic Processing Unit) based architecture.

A decrease of two orders of magnitude of the processing time was obtained by MUMPS, in comparison to the LTS_N implementation that uses

the LAPACK solver. In addition, the solution of the MUMPS method converged. However, due to the ill-conditioning of the system matrix, the solutions of the iterative methods did not converge and processing times were high. The discussion about processing times and convergence attaioned by the different solvers is shown in Section 3.

The performance optimization of the LTS_N method is focused in this work since it is employed for solving hydrologic optics inverse problems in an implicit way, which demands hundreds or thousands of executions of the LTS_N method itself.

2   Radiative Transfer Equation

The Radiative Transfer Equation (RTE) for radiances L is given by

$$
\mu \frac{\partial}{\partial \tau} L(\tau, \mu, \varphi) + L(\tau, \mu, \varphi) =
$$

$$
\frac{\varpi_0(\tau)}{4\pi} \int_{-1}^{1} \int_{0}^{2\pi} \beta(\mu, \varphi; \mu', \varphi') L(\tau, \mu', \varphi') d\varphi' d\mu'
$$
$$
+ S(\tau, \mu, \varphi)
$$

(1)

where τ is the optical depth, $\mu \in [-1, 1]$ and $\varphi \in [0, 2\pi]$ are the cosine of the incident polar angle θ and the incident azimuthal angle, respectively. ϖ_0 is the constant single scattering albedo. The scattering phase function $\beta(\mu, \varphi; \mu', \varphi')$, gives the scattering beam angular distribution and the source term is $S(\tau, \mu, \varphi)$.

2.1   The discrete ordinates method

In a non-homogeneous medium with N_g degrees of anisotropy, the scattering angle is then discretized into $(N_g + 1)$ azimuthal modes, with N polar angles, while the domain is splitted into R homogeneous regions. The radiate transfer equation is then expressed as the discrete ordinate equations, also

known as S_N equations, given by

$$\mu_j \frac{d}{d\tau} L_r^m(\tau, \mu_j) + L_r^m(\tau, \mu_j) =$$

$$\frac{\varpi_r}{2} \sum_{l=m}^{N_g} \beta_l^m P_l^m(\mu_j) \sum_{i=1}^{N} \eta_i P_l^m(\mu_i) L_r^m(\tau, \mu_i)$$

$$+ S_r^m(\tau, \mu_j),$$

$$j = 1, 2, \ldots, N$$

$$m = 0, 1, 2, \ldots, N_g$$

$$r = 0, 1, 2, \ldots, R$$

$$\tag{2}$$

The boundary conditions are

$$L_1^m(0, \mu_j) = 0 \quad j = 1, 2, \ldots, n \tag{3a}$$

$$L_R^m(\tau_R, -\mu_j) = 0 \quad j = n+1, n+2, \ldots, N. \tag{3b}$$

2.2   The LTS$_N$ approach

The LTS$_N$ method [4, 8] applies the Laplace transform on the radiative transfer discrete ordinates equations, given by (2) and (3). This yields a system of symbolic algebraic equations on s:

$$s\overline{L}_{j,r}^m(s) + \frac{1}{\mu_j} \overline{L}_{j,r}^m(s) -$$

$$\frac{\varpi_r}{2\mu_j} \sum_{l=m}^{L} \beta_l^m P_l^m(\mu_j) \sum_{i=1}^{N} \eta_i P_l^m(\mu_i) \overline{L}_{i,r}^m(s) =$$

$$L_{j,r}^m(0) + \frac{1}{\mu_j} \overline{S}_{j,r}^m(s) \tag{4}$$

where $\overline{L}_{j,r}^m(s) = \int_0^\infty L_{j,r}^m(\tau) e^{-s\tau} \, d\tau$. The matrix form of equation (4) becomes

$$\overline{M}_{N,r}^m(s) \overline{L}_r^m(s) = L_r^m(0) + \overline{Q}_r^m(s). \tag{5}$$

where the N-order matrix $\overline{M}_{N,r}^m(s)$, called the LTS$_N$ matrix, is given by

$$\overline{M}_{N,r}^m(s) = s\mathbf{I} + A_r^m \tag{6}$$

and **I** is the N-order identity matrix, while the A^m matrix is given by

$$
a_r^m(i,j) = \begin{cases} \dfrac{1}{\mu_j} - \dfrac{\varpi_r}{2\mu_j} \sum_{l=m}^{L} \beta_l^m P_l^m(\mu_j)\eta_j P_l^m(\mu_j), \\ \qquad\qquad\qquad\qquad \text{if } i = j, \\ \\ -\dfrac{\varpi_r}{2\mu_j} \sum_{l=m}^{L} \beta_l^m P_l^m(\mu_j)\eta_i P_l^m(\mu_i), \\ \qquad\qquad\qquad\qquad \text{if } i \neq j. \end{cases}
\tag{7}
$$

and vectors $\overline{L}_r^m(s)$, $L_r^m(0)$ and $\overline{Q}_r^m(s)$ are defined as

$$
\overline{L}_r^m(s) = \left[\overline{L}_{1,r}^m(s)\ \overline{L}_{2,r}^m(s)\ \ldots\ \overline{L}_{N,r}^m(s) \right],
$$

$$
\overline{L}_r^m(0) = \left[\overline{L}_{1,r}^m(0)\ \overline{L}_{2,r}^m(0)\ \ldots\ \overline{L}_{N,r}^m(0) \right],
$$

$$
\overline{Q}_r^m(s) = \left[\dfrac{\overline{S}_{1,r}^m(s)}{\mu_1}\ \dfrac{\overline{S}_{2,r}^m(s)}{\mu_2}\ \ldots\ \dfrac{\overline{S}_{N,r}^m(s)}{\mu_N} \right].
$$

In order to solve the matrix equation (5), it must be multiplied by the inverse matrix of $\overline{M}_{N,r}^m(s)$, as follows

$$
\overline{L}_r^m(s) = \left[\overline{M}_{N,r}^m(s) \right]^{-1} L_r^m(0) + \left[\overline{M}_{N,r}^m(s) \right]^{-1} \overline{Q}_r^m(s),
\tag{8a}
$$

$$
\overline{L}_r^m(s) = \overline{B}_r^m(s) L_r^m(0) + \overline{B}_r^m(s)\overline{Q}_r^m(s).
\tag{8b}
$$

Applying the Laplace inverse transform

$$
L_r^m(\tau) = B_r^m(\tau) L_r^m(0) + H_r^m(\tau)
\tag{9}
$$

where

$$
B_r^m(\tau) = \mathcal{L}^{-1}\left[\overline{B}_r^m(s) \right]
\tag{10}
$$

and

$$
H_r^m(\tau) = B_r^m(\tau) * Q_r^m(\tau)
\tag{11}
$$

where the convolution is denoted by $*$.

The implementation of the LTS$_N$ method solves each mth azimuthal-mode system of order $R \times N$ shown in Equation (9), for $m = 0, 1, 2, \ldots, N_g$, R regions and Nth-order of quadrature.

Applying in Equation (9), the boundary conditions and a criterion of continuity between adjacent regions, i.e., $L_r^m(\tau) = L_{r+1}^m(0)$, yields to the systems given by the Equation (12)

$$
\begin{bmatrix}
\mathtt{B}_{11}^{(1)}(0)\mathtt{B}_{12}^{(1)}(0) & & & & \\
\mathtt{B}^{(1)}(\tau_1) & -\mathtt{B}^{(2)}(0) & & & \\
& \mathtt{B}^{(2)}(\tau_2) & -\mathtt{B}^{(3)}(0) & & \\
& & & \ddots & \\
& & & \mathtt{B}^{(R-1)}(\tau_{R-1}) & -\mathtt{B}^{(R)}(0) \\
& & & & \mathtt{B}_{21}^{(R)}(\tau_R)\mathtt{B}_{22}^{(R)}(\tau_R)
\end{bmatrix}
\begin{bmatrix}
L_1 \\ L_2 \\ L_3 \\ \vdots \\ L_{R-1} \\ L_R
\end{bmatrix}
=
$$

$$
=
\begin{bmatrix}
-H_1^d(0) \\
H_2(0) - H_1(\tau_1) \\
H_3(0) - H_2(\tau_2) \\
\vdots \\
H_R(0) - H_{R-1}(\tau_{R-1}) \\
-H_R^u(\tau_R)
\end{bmatrix}
$$

$$(12)$$

For instance, Figure 1 shows the sparse structure of the linear system matrix given by the Equation (12), for a non-homogeneous medium with 10 regions and 50 polar directions. This yields to a matrix with 500 rows and columns, containing 47500 nonzero elements (nnz=47500).

3   Results

The computational performance of the original implementation of the LTSN method, which employs the LAPACK solver was taken as reference [3],which was developed for dense matrices. The considered case study refers to a non-homogeneous medium, with 80 depth regions and 150 polar directions. The resulting sparse linear system has 12000 unknown radiances, and its linear system matrix has 3577000 nonzero elements (nnz = 3577500). Figure 2 shows the matrix of this case study.

The other direct solver tested for the case study problem is the one of the MUMPS library (MUltifrontal Massively Parallel sparse direct solver) [1, 2], which is specific for sparse matrices. The iterative solvers tested here were the GMRES method implemented in the LIS library [7], specific for multi-core CPUs, and the CUSP package [5], developed for GPU-based architectures.

Computational performance tests were performed in a cluster node that includes two octacore Intel Xeon E5-2660 (Sandy Bridge, 2.2GHz) processors

Matrix of LTSn. 50 directions and 10 regions (500 x 500)
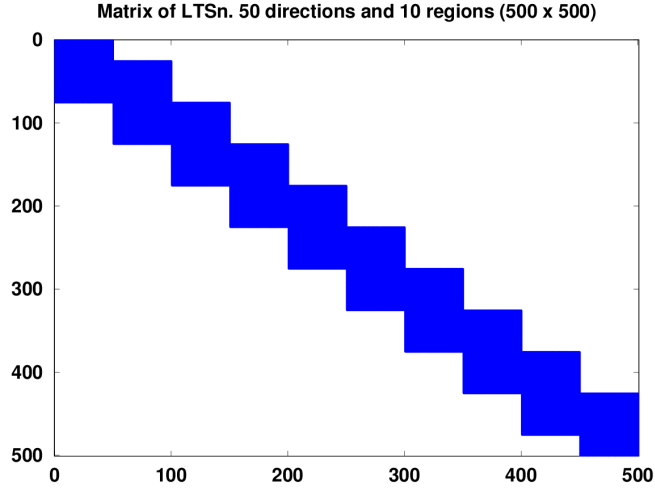
Figure 1: Sparse structure of the linear system matrix, considering a non-homogeneous medium with 10 regions and 50 polar directions
Size=500 and nnz=47500

and a GPU NVIDIA Tesla K20m. Main memory is 64 GB and GPU memory, 5GB. The performance of the different methods is shown in Table 1.

Direct methods were successfull in finding the system solution, but the execution time of the MUMPS package solver was about 100 times lower than the reference solver of the LAPACK library. This improved performance was indeed expected, since MUMPS is a specific solver for sparse systems.

On the contrary, although the iterative GMRES methods from LIS (CPU) and CUSP (GPU) packages demanded execution times similar the MUMPS solver, they were not able to achieve the system solution. In fact, both failed to converge to the solution, even after 200 iterations. This behavior can be attributed to the ill-conditioning of the linear system matrix. The stop criterion adopted was the relative residual 2-norm lower than 10^{-6}, i.e., $tolerance = \|x^2\| < 10^{-6}$, or number of iterations up to 200.
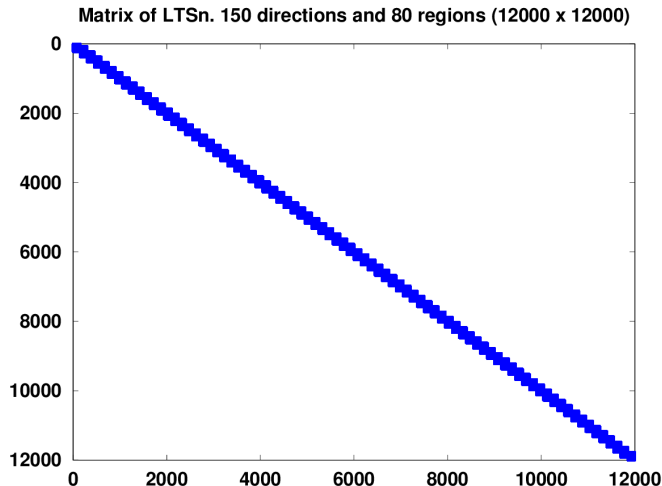
Figure 2: Sparse structure of the linear system matrix, considering a non-homogeneous medium with 80 regions and 150 polar directions. Size=12000 and nnz=3577500

Solver	Time(s)	Iterations	Relative residual 2-norm
LAPAPACK/DGETRF	56.34	-	-
MUMPS	0.52	-	-
LIS/GMRES	1.02	200	9.96E-001
CUSP/GMRES	0.40	200	3.83E-001

Table 1: Execution time of direct and iterative methods

4   Final Remarks

This work aimed at the optimization performance of the LTS_N method by chosing a solver more suited for sparse linear systems. This goal was achieved using the direct method implemented in MUMPS package, that obtained for the case study problem a decrease of about two orders of magnitude in comparison to the LAPACK solver originally implemented in the LTS_N method.

However, the two iterative methods tested here, intended for multicore and GPU architectures, failed to achieve the solution for the case study problem, mainly due to the ill-conditioning of the LTS_N linear system ma-

trix. A further study will exploit the use of suitable preconditioners for these methods.

The improvement of the computational performance is critical in the case of inverse problems that estimate optical properties of the medium, since they are solved implicitly by formulating the inverse problem as an optimization one. In an iterative process, each candidate solution composed of guessed values is evaluated by the radiative transfer equation (RTE) yielding a light field that is compared to the measurements by the corresponding quadratic difference. A stochastic optimizer is used to generate the candidate solution for the next iteration [9, 6, 12]

It is worth to note that hundreds or even more of iterations of the inverse solver for complex cases may demand processing times that may be unfeasible, especially for problems that involve anisotropic and non-homogeneous medium with very vertical levels [10, 11], as shown here, justifying the research for a better performance of the LTS$_N$ method by improving its linear system solver.

References

[1] Amestoy, P. R., Duff, I. S., Koster, J., and L'Excellent, J.-Y. A fully asynchronous multifrontal solver using distributed dynamic scheduling. *SIAM Journal on Matrix Analysis and Applications 23*, 1 (2001), 15–41.

[2] Amestoy, P. R., Guermouche, A., L'Excellent, J.-Y., and Pralet, S. Hybrid scheduling for the parallel solution of linear systems. *Parallel Computing 32*, 2 (2006), 136–156.

[3] Anderson, E., Bai, Z., Bischof, C., Blackford, S., Dongarra, J., Du Croz, J., Greenbaum, A., Hammarling, S., McKenney, A., and Sorensen, D. *LAPACK Users' guide*, vol. 9. Siam, 1999.

[4] Barichello, L. B., and Vilhena, M. T. A general approach to one-group one-dimensional transport equation. *Kerntechnik 58*, 3 (1993), 182–184.

[5] Bell, N., and Garland, M. Cusp: Generic parallel algorithms for sparse matrix and graph computations. *Version 0.3.0 35* (2012).

[6] Carvalho, A., de Campos Velho, H., adn R.P. Souto, S. S., Becceneri, J., and Sandri, S. Fuzzy ant colony optimization for estimating chorophyll concentration profile in offshore sea water. *Inverse Problems in Science and Engineering 16*, 6 (2008), 705–715.

[7] Nishida, A. Experience in developing an open source scalable software infrastructure in japan. In *International Conference on Computational Science and Its Applications* (2010), Springer, pp. 448–462.

[8] Segatto, C. F., and Vilhena, M. T. Extension of the ltsn formulation for discrete ordinates problem without azimuthal symmetry. *Annals of Nuclear Energy 21*, 11 (1994), 701–710.

[9] Souto, R. P., CamposVelho, H. F., Stephany, S., and Sandri, S. Estimating vertical chlorophyll concentration in offshore ocean water using a modified ant colony system. *Journal of Mathematical Modelling and Algorithms (JMMA)* (2006).

[10] Souto, R. P., Dias, P. L. S., CamposVelho, H. F., Stephany, S., and Kampel, M. Reconstruction of chlorophyll-a vertical profiles with enhanced resolution. In *Proceedings of 10th World Congress on Computational Mechanics* (São Paulo, 2012).

[11] Souto, R. P., Dias, P. L. S., Velho, H. F. C., Stephany, S., and Kampel, M. New developments on reconstruction of high resolution chlorophyll-a vertical profiles. *Computational and Applied Mathematics*, 1–10.

[12] Stephany, S., Becceneri, J., Souto, R., de Campos Velho, H., and Silva Neto, A. A pre-regularization scheme for the reconstruction of a spatial dependent scattering albedo using a hybrid ant colony optimization implementation. *Applied Mathematical Modelling 34*, 3 (2010), 561–572.